Frequency Calibration of Terahertz Time-Domain Spectrometer Using Air-Gap Etalon

Moto Kinoshita, Hitoshi Iida, and Yozo Shimada

***Abstract*—Although various terahertz (THz) technologies have been rapidly developed in recent years, their metrology standards are yet to be established. We have developed a simple calibration method for the frequency of a THz time-domain spectrometer (TDS) using an optically transparent THz air-gap etalon (OT-TAGE). The OT-TAGE can be used in both the near-infrared (NIR) and THz regions. Therefore, a frequency measurement using THz waves can be directly compared with one using NIR light via the OT-TAGE. In this study, the frequency of a commercial THz-TDS was calibrated by referring to the NIR wavelength was demonstrated. The obtained frequency errors were within ±3 GHz, with relative uncertainties within 1%.**

***Index Terms*—Time-domain analysis, frequency, air gaps, interferometers, calibration.**

IN CONSTRAST to radio waves and optics, which have seen widespread applications over the years, applications of terahertz (THz) waves, such as imaging, communications, and spectroscopy, have been developed only recently. In particular, the THz time-domain spectrometer (THz-TDS) is commonly used for analytic applications. However, metrology standards, which are essential for the public utilization of THz technologies, are yet to be established. The frequency standards as well as linearity and power standards are important for the THz-TDS [1]–[4]. For example, security and medical analyses require the frequency standards to share fingerprint spectra measured by different devices and operators. Although the THz frequency comb is promising as a frequency standard [5], it is only available in the few laboratories equipped with an optical frequency comb. While the absorption lines of standard gases contained in databases are used for practical calibration, establishing metrological traceability is challenging. Etalon-based calibration, which is expected to be superior to the H_2O-gas-based method, has been also suggested [6], [7]. The etalon is a simple resonator and consists of two reflection planes. It is practical and compact, which means that it can be used as a simple tool for obtaining a frequency reference. Its transmittance has equally spaced peaks due to interference from the multiple reflections between the two planes. The interval between each peak, namely, the free spectral range (FSR), can be written as

$$\mathrm{FSR} = \frac{c}{2nL} \tag{1}$$

where, c is the speed of light, and n and L are, respectively, the refractive index and length of the resonant cavity of the etalon. In the case of a solid etalon, accurate measurement of n or estimation of its uncertainty is required [6], [7]. However, it has proven difficult to verify the absolute value of n and to evaluate its uncertainty. In contrast, the value of n of an air-gap etalon, which has an air-filled cavity, can be approximated to 1 [8]. According to (1), the FSR of an air-gap etalon depends only on L. Therefore, if L can be precisely measured, air-gap etalons can potentially be used as simple tools for frequency calibration and verification in various THz applications. An optical method is typically used for measuring lengths. Although an air-gap etalon made of two Si wafers has been proposed [7], optical measurement of the cavity length is not possible for such an opaque etalon. With these considerations, we have developed an air-gap etalon that can transmit both THz waves and near-infrared (NIR) light. NIR light enables the FSR of the air-gap etalon (i.e., L) to be measured using an optical method. Then, the optically measured FSR can be used for the frequency calibration of THz waves. Optically transparent THz air-gap etalons (OT-TAGEs) made of Inconel-evaporated plates were fabricated in previous studies. We previously directly compared the FSRs obtained using THz and NIR measurements and confirmed the feasibility of OT-TAGEs [9], [10], in which a THz-TDS based on mechanical time-delay scanning was used. However, the optical measurement using the Inconel-OT-TAGE was not accurate enough to achieve the frequency calibration. In this study, we developed a new OT-TAGE consisting of Ag-evaporated plates to improve the resolution and accuracy of frequency measurement. The frequency calibration of a commercial THz-TDS using the new OT-TAGE was demonstrated, for which the uncertainties were evaluated. The transmittance of the Ag-OT-TAGE is expected to be too low to apply to a usual THz-TDS. Therefore, the THz-TDS based on the asynchronous optical sampling method (ASOPS) [11] was used in this study. However, this low transmittance of the Ag-OT-TAGE can be improved by adjusting thickness of Ag membrane. The frequency calibration of a THz-TDS based on mechanical scanning using an optimized Ag-OT-TAGE will be demonstrated in future work.

Using the FSR measured with NIR light, namely, $\mathrm{FSR_{NIR}}$, the frequency measured in the THz region f_{THz} can be written as

$$f_{\mathrm{THz}} = N \times \mathrm{FSR_{NIR}} + f_{\mathrm{offset}}. \tag{2}$$

Here, N is the index number of the Nth peak in the transmittance of the OT-TAGE in the order of increasing frequency and f_{offset} is the offset frequency caused by the phase shift induced

Manuscript received June 29, 2014; revised August 05, 2014; accepted September 08, 2014. Date of publication September 19, 2014; date of current version October 30, 2014.

The authors are with National Metrology Institute of Japan (NMIJ), National Institute of Advanced Industrial Science and Technology (AIST), Tsukuba, Japan (e-mail: moto-kinoshita@aist.go.jp, h-iida@aist.go.jp, and yozo.shimada@aist.go.jp).

Digital Object Identifier 10.1109/TTHZ.2014.2357895

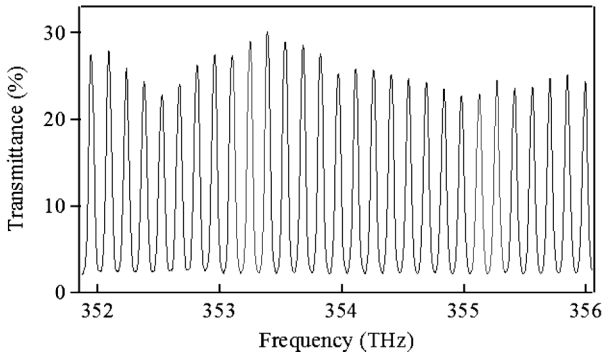

Fig. 1. Transmittance of the OT-TAGE measured in the NIR region. $\mathrm{FSR_{NIR}}$ was estimated to be 144.476 GHz ±0.032 GHz by FFT analysis.

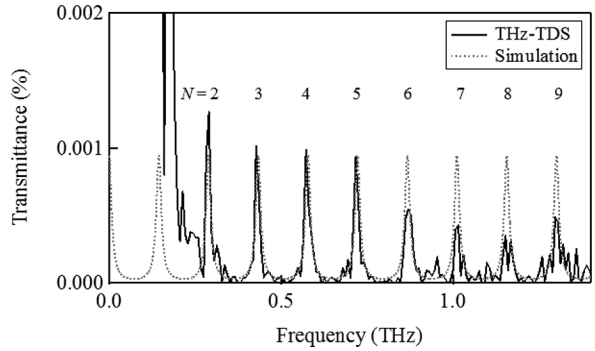

Fig. 2. Transmittance of the OT-TAGE measured in the THz region using a THz-TDS. The peaks from $N = 2$ to $N = 9$ are labeled.

by the reflection. This method has the potential for easy calibration and verification of the frequency measurement using a THz-TDS that is traceable to the optical wavelength.

The OT-TAGE was fabricated by setting two Ag-evaporated plates made of cycloolefin polymer facing each side of a membrane across a glass ring-type spacer. The ring-type spacer provides an air-gap cavity. THz waves and NIR light can penetrate the cycloolefin polymer and Ag membranes. Therefore, if n is constant, the FSRs in the THz and NIR regions should be equal. The thickness of the ring-type spacer L was nominally 1 mm. The actual value of L can be estimated using FSR measurement with NIR light.

The FSR of the OT-TAGE in the NIR region was evaluated using a transmission measurement system consisting of a broadband superluminescent diode (SLD), focusing and collimating lenses, and an optical spectrum analyzer. NIR light with a wavelength of approximately 850 nm emitted from the SLD was collimated by the optical lens and transmitted to the OT-TAGE. After transmission, it was detected by the optical spectrum analyzer with the use of the focusing lens. The obtained transmittance of the OT-TAGE is shown in Fig. 1. The finesse of the OT-TAGE was evaluated to be 2.8 from Fig. 1. $\mathrm{FSR_{NIR}}$ was estimated using fast Fourier transformation (FFT) of the periodic peaks of the transmittance shown in Fig. 1. The obtained value with the standard deviation was 144.476 GHz ± 0.032 GHz, which corresponds to $L = 1037.52\ \mu\mathrm{m} \pm 0.23\ \mu\mathrm{m}$. Length measurement with this accuracy is difficult to achieve with a mechanical method because of the uncertainties in measuring the thickness, evaluating the flatness, and correcting the distortion resulting from the assembly.

A commercial THz-TDS (TAS7500SP, Advantest Corp.) based on the ASOPS was calibrated by referring to the above measured value of $\mathrm{FSR_{NIR}}$. The ASOPS-THz-TDS has two photoconductive antennas (PCAs) as its emitter and detector and two femtosecond (fs) pulse lasers with slightly different pulse repetition frequencies. This frequency difference provides a timing delay between THz wave emission and detection upon exciting the PCAs. The THz pulse emitted by one of the PCAs was guided and focused into the OT-TAGE and then detected by the other PCA. After FFT analysis of the time-domain spectrum, which was obtained using the detecting PCA via the timing delay, the frequency domain spectrum was calculated. The transmittance of the OT-TAGE in the THz region is shown as a solid line in Fig. 2, in which peaks from $N = 2$ to $N = 9$ are labeled. The peaks with an index number of 1 and greater than 10 were vague because of the poor signal-to-noise ratio (SNR) that resulted from the low transmittance, i.e., less than 0.002%. The SNR can be improved by thinning the Ag membrane. The OT-TAGE with a higher SNR has applications that are more practical. However, note that the thickness of the Ag membrane must be carefully adjusted because of a trade-off between the SNR and finesse. The finesse of the OT-TAGE was evaluated to be 8.5 from Fig. 2. The dotted line represents transmittance simulated with an FSR of 144.476 GHz and finesse of 8.5. The disagreement of the peak amplitude between the measurement and simulation at high frequencies resulted from THz losses in the OT-TAGE. The frequency calibration of the THz-TDS based on the OT-TAGE was achieved by evaluating the frequency error, which is defined as the difference between each peak position of the transmittance of the OT-TAGE measured using the THz-TDS and the corresponding frequency obtained from (2) using the measured $\mathrm{FSR_{NIR}}$.

To estimate the frequency error, the offset frequency f_{offset} caused by a phase shift must be evaluated. In this study, the phase shift induced by reflection at the Ag membranes was assumed to be π and its uncertainty was evaluated. If the phase shift δ is a linear function of the frequency f, it can be written as

$$\delta(f) = \delta_0 \pm u(\delta_0) + \{\delta_1 \pm u(\delta_1)\}\, f. \tag{3}$$

Here, we assume that $\delta_0 = \pi$ and $\delta_1 = 0$, but their uncertainties $u(\delta_0)$ and $u(\delta_1)$ have nonzero values. The values of $u(\delta_0)$ and $u(\delta_1)$ were estimated using reflection measurements with a THz reflectometer consisting of a movable mirror, a fs pulse laser, and two PCAs. The fs pulse was split into two beams, one of which was given a timing delay using a movable mirror. The Ag-evaporated cycloolefin polymer was placed in the path of the focused THz beam emitted by one of the PCAs, and the reflected waves were detected. The phase of the reflected waves was calculated through FFT analysis of the reflection spectrum in the time domain. Then, the phase shift caused by the reflection at the Ag membrane was estimated as the phase difference between the reflections at the Ag membrane and cycloolefin plane as a reference shift of π. The measured phase shifts due to the reflection at the two Ag membranes (#1 and #2) are shown in

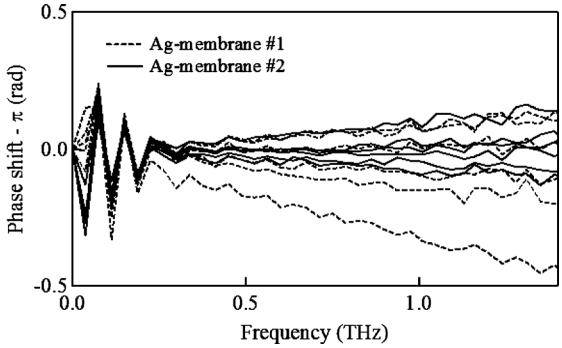

Fig. 3. Phase shifts caused by reflection at the Ag membranes shown as the difference from π. The uncertainties of δ_0 and δ_1 were estimated.

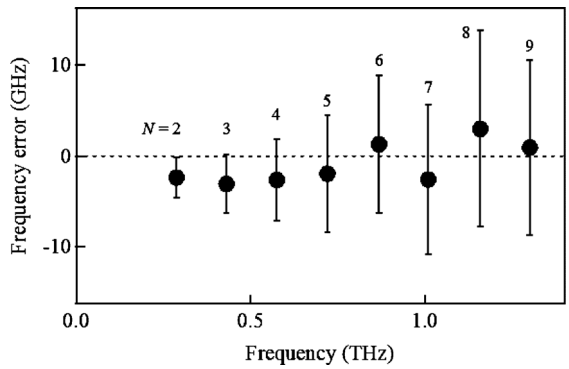

Fig. 4. Frequency errors between measurements with a THz-TDS and an NIR transmission system. These results demonstrate the accuracy of the THz-TDS.

Fig. 3 as the difference from the reference shift of π. Six measurements were made for each membrane. The phase shifts appear to vary around $\delta_0 = \pi$ and $\delta_1 = 0$ in accordance with our assumption. By fitting each phase shift in Fig. 3 with a linear function of the frequency f and calculating their standard deviations, $u(\delta_0)$ and $u(\delta_1)$ were estimated to be 0.015 rad and 0.128 rad/THz, respectively.

While the offset frequency $f_{\rm offset}$ was equal to zero under the assumption that $\delta_0 = \pi$ and $\delta_1 = 0$, its uncertainty $u(f_{\rm offset})$ was estimated using

$$u(f_{\rm offset}) = \frac{u(\delta_0)}{\pi}{\rm FSR_{NIR}}. \tag{4}$$

In addition, the uncertainty of $\rm FSR_{NIR}$ as a result of the phase shift $u_{\rm PS}({\rm FSR_{NIR}})$ is written as

$$u_{\rm PS}({\rm FSR_{NIR}}) = \frac{u(\delta_1)}{\pi}{\rm FSR_{NIR}^2}. \tag{5}$$

Substituting $u(\delta_0) = 0.015$ rad and $u(\delta_1) = 0.128$ rad/THz into (4) and (5), respectively, the uncertainties $u(f_{\rm offset})$ and $u_{\rm PS}({\rm FSR_{NIR}})$ were evaluated to be 0.711 and 0.848 GHz, respectively.

The other factors contributing to the uncertainty of $\rm FSR_{NIR}$ were the angle of incidence of the NIR beam into the OT-TAGE, the accuracy of the spectrum analyzer, and the refractive index of air. The angle of incidence was estimated to be less than $\tan^{-1}(1.5/420)$ after geometrical analysis. This corresponds to an uncertainty of 921 kHz for the $\rm FSR_{NIR}$ of 144.476 GHz. The accuracy of the optical spectrum analyzer was estimated using a stable laser, the wavelength of which was stabilized to the absorption line of a cesium atom. The established wavelength of the D_2 line of cesium, from the $F = 4$ to $F' = 4$ transition, is 852.357 nm [12], while the value measured with the spectrum analyzer was 852.332 nm. Thus, the uncertainty associated with the spectrum analyzer was estimated to be 2.54 MHz. The difference between the refractive indices of air in the NIR and THz regions was estimated to be less than 2.31×10^{-6} by referring to the wavelength of 800 nm and the limiting value at infinity in [8]. This corresponds to an uncertainty of 333 kHz. The combined uncertainty of $\rm FSR_{NIR}$ was evaluated as the root sum square of the above uncertainties, which includes the standard deviation of 0.032 GHz and the phase-shift uncertainty of 0.848 GHz. The value obtained was 0.849 GHz, which corresponds to a relative standard uncertainty of 0.6%.

Using ${\rm FSR_{NIR}} = 144.476$ GHz $\pm$ 0.849 GHz and $f_{\rm offset} =$ 0 GHz $\pm$ 0.711 GHz, the frequency errors at the peaks of the transmittance of the OT-TAGE from $N = 2$ to $N = 9$ were obtained as shown in Fig. 4. The frequency errors in Fig. 4 were evaluated as the average of three repeated measurements. The uncertainties of the frequency errors were evaluated as the root sum square of the uncertainty of $\rm FSR_{NIR}$ multiplied by N, that of $f_{\rm offset}$, and the standard deviation of the three repeated measurements. Since this uncertainty is an increasing function of N, it increases at higher frequency. The relative expanded uncertainties at a coverage factor of 2, which corresponds to twice the standard uncertainty, were within 1%. The frequency errors demonstrate the accuracy of the THz-TDS under test. The frequency errors in Fig. 4 were within ± 3 GHz. Nevertheless, considering the frequency errors and their uncertainties, these results are consistent with the fact that the frequency resolution and accuracy of the THz-TDS under test, which were taken from its specifications, were, respectively, 7.6 GHz and 10 GHz.

In conclusion, a simple and practical method for calibrating the frequency measurement of a THz-TDS based on an OT-TAGE was demonstrated. Since an OT-TAGE can be utilized in the THz and NIR regions, this frequency calibration is traceable to the wavelength of NIR light. The frequency errors of the THz-TDS under test, which indicate the accuracy of the frequency measurements, were within ± 3 GHz. The relative expanded uncertainties were within 1%.

ACKNOWLEDGMENT

The authors would like to thank Advantest Corporation for their help with the THz-TDS.

REFERENCES

[1] L. Werner, H. W. Hübers, P. Meindl, R. Müller, H. Richter, and A. Steiger, "Towards traceable radiometry in the terahertz region," *Metrologia*, vol. 46, no. 4, pp. S160–S164, 2009.

[2] M. Naftaly and R. Dudley, "Linearity calibration of amplitude and power measurements in terahertz systems and detectors," *Opt. Lett.*, vol. 34, no. 5, pp. 674–676, 2009.

[3] H. Iida, M. Kinoshita, Y. Shimada, H. Kuroda, K. Kitagishi, and Y. Izutani, "Validation of power linearity in terahertz time-domain spectroscopy using a programmable step attenuator," *IEEE Trans. Instrum. Meas.*, vol. 62, no. 6, pp. 1801–1806, Jun. 2013.

[4] H. Iida, M. Kinoshita, and Y. Shimada, "Calorimetric measurement of absolute terahertz power at the sub-microwatt level," *Opt. Lett.*, vol. 39, no. 6, pp. 1609–1612.
[5] T. Yasui, Y. Kabetani, and E. Saneyoshi, "Terahertz frequency comb by multifrequency-heterodyning photoconductive detection for high-accuracy, high-resolution terahertz spectroscopy," *Appl. Phys. Lett.*, vol. 88, p. 241104, 2006.
[6] M. Naftaly, R. A. Dudley, J. R. Fletcher, F. Bernard, C. Thomson, and Z. Tian, "Frequency calibration of terahertz time-domain spectrometers," *J. Opt. Soc. Amer. B*, vol. 26, no. 7, pp. 1357–1362, 2009.
[7] M. Naftaly, R. A. Dudley, and J. R. Fletcher, "An etalon-based method for frequency calibration of terahertz time-domain spectrometers (THz TDS)," *Opt. Commun.*, vol. 283, pp. 1849–1853, 2010.
[8] R. Penndorf, "Table of the refractive index for standard air and the Rayleigh scattering coefficient for the spectral region between 0.2 and 20.0 μ and their application to atmospheric optics," *J. Opt. Soc. Amer.*, vol. 47, no. 2, pp. 176–182, 1957.
[9] M. Kinoshita, H. Iida, Y. Shimada, H. Kuroda, K. Kitagishi, and Y. Izutani, "Development of compatible air-gap etalons used with both terahertz wave and near-infrared light," in *Proc. 37th IRMMW-THz, PB-1*, 2012.
[10] M. Kinoshita, H. Iida, and Y. Shimada, "Direct comparison between frequencies measured in terahertz and near infrared ranges," in *Ext. Abst. OTST 2013*, 2013, p. 192.
[11] T. Yasui, E. Saneyoshi, and T. Araki, "Asynchronous optical sampling terahertz time-domain spectroscopy for ultrahigh spectral resolution and rapid data acquisition," *Appl. Phys. Lett.*, vol. 87, p. 061101, 2005.
[12] D. A. Steck, "Cesium D line data," May 2008 [Online]. Available: http://steck.us/alkalidata, revision 2.0.1.